8$^{\text{th}}$ International Cloud Modelling Workshop
Case 1: CCN processing by a drizzling stratocumulus

Organized by Wojciech Grabowski (NCAR/MMM) and Zach Lebo (NCAR/ASP)

version of: August 15, 2012

1   Overview

The purpose of this case is to investigate accuracy and efficiency of various approaches to simulate processing of CCN by precipitating clouds. The motivation comes from observed dramatic differences between aerosol characteristics between areas of closed and open cells within stratocumulus over subtropical eastern Pacific. The problem is important because open and closed cells have dramatically different cloud characteristics, with almost 100% cloud cover for the closed cells and significantly lower (below 20%) cloud cover for the open cells. CCN processing at the boundary between open and closed cells has been argued to play an important role, perhaps even control, the transition from open- to closed-cell circulations.

2   Case description

The specific modeling case described here is based on observations of drizzling stratocumulus. Two separate modeling approaches are considered, the prescribed-flow (kinematic model) case, and the two-dimensional (2D) dynamic airflow model, both focusing on microphysical processes within drizzling stratocumulus. Each participant is expected to use both frameworks and prepare the results using the guidelines discussed below. However, using only one of the frameworks is also acceptable.

The setup for both dynamic and kinematic cases is based on VOCALS observation of subtropical drizzling stratocumulus. Idealized profiles of the total water and liquid water potential temperature are used to specify the initial profiles for the model simulations. Initial CCN characteristics are also base on VOCALS observations. In both kinematic and dynamic model simulations, the emphasis is on the representation of CCN processing by the drizzling stratocumulus and on the gradual increase of the drizzle rate as a result of reduction of total CCN number and modification of CCN size distribution.

The initial liquid water potential temperature, θ_l, and the total water mixing ratio profiles, q_t are prescribed as:

$$\theta_l = \begin{cases} 289.0 & \text{for } z \leq z_{inv}^0 \\ 303.0 + (z - z_{inv}^0)^{1/3} & \text{for } z > z_{inv}^0 \end{cases}$$

$$q_t = \begin{cases} 7.5 & \text{for } z \leq z_{inv}^0 \\ 0.5 & \text{for } z > z_{inv}^0 \end{cases}$$

where $z_{inv}^0 = 1500m$ is the initial inversion height. Note that z_{inv}^0 is also the depth of the kinematic model computational domain and only profiles below that height (i.e., constant θ_l and q_t) are used as initial profiles in the kinematic model. When decomposing the profiles into profiles of the potential temperature, water vapor and cloud water mixing ratio, the hydrostatic pressure profile has to be used assuming the surface pressure of 1015 hPa. The initial profiles represent the well-mixed stratocumulus-topped boundary layer with a cloud extending from the cloud base at approximately 950 m to the boundary-layer inversion at 1500 m.

For simplicity we assume that the aerosols are amonium sulfates with the initial dry aerosol spectrum given by two-mode lognormal aerosol size distribution following observations reported in Wood et al. (2011, Figs. 15 and 16 therein) and Allen et al. (2011, Table 4 therein), but with low concentrations to initiate quickly aerosol processing. The parameters for the initial distributions for the the two modes are the total concentrations of 60 and 40 cm^{-3}, mean radii of 0.04 and 0.15 μm, and geometric standard deviations of 1.4 and 1.6 for the first and second mode, respectively.

3   Kinematic Model simulations

The kinematic model computational domain is 1500 x 1500 m^2, the gridlength is 20 m in both directions, and the grid is 75 x 75. The prescribed velocity field represents a single eddy spanning the entire extent of the computational domain and featuring the maximum vertical velocity of about 1 m s^{-1}, see Fig. 1. To maintain steady mean temperature and moisture profiles (i.e., to compensate for gradual water loss due to precipitation and warming of the boundary layer due to latent heating), mean temperature and moisture profiles are relaxed to the initial profiles with a height-dependent relaxation time scale $\tau = \tau_{rlx}\exp(z/z_{rlx})$, with $\tau_{rlx} = 300s$ and $z/z_{rlx} = 200m$ (i.e., temperature and moisture equations have an additional source in the form $(\psi_i < \psi >)/\tau_{rlx}$ where ψ_i is the initial profile and $< \psi >$ is the horizontal mean of ψ at a given height. Note that such a formulation does not dump small-scale perturbations of ψ, but simply shifts the horizontal mean toward ψ_i. Such a term mimics the effects of surface fluxes that maintain the balance in the natural case.

The initial simulations should only consider activation/coalescence scavenging, that is, the change of CCN spectrum due to drizzle should only include processes associated with CCN activation, droplet collisional growth, drizzle fallout and either below-cloud evaporation or loss when reaching the surface. Additional processes, such as, for instance, scavenging of unactivated (interstitial) CCN within the cloud (through the interaction with cloud droplets) or scavenging by falling drizzle below the cloud, may be added to compare their impact with the activation/coalescence scavenging. Some discussion of these processes is given in Flossmann and Wobrock (2010), although not focusing specifically on stratocumulus.

We anticipate that a variety of schemes will be put to the test of the kinematic model. Arguably the benchmark will be provided by a two-dimensional bin scheme (droplet radius times aerosol mass). Bin model with simplified representation of CCN will be used by some. A double-moment microphysics with possibly double-moment CCN representation will serve as a computationally-efficient approach, and exploring how accurate such an approach is to represent aerosol processing is one of particular goals of this case.

The FORTRAN 77 source code linked here[1] can be used for the kinematic model and a new modular microphysics scheme can be readily replaced into this code by individual developers of similar routines. It has a bulk representation of the microphysics without CCN processing, and has to be adopted to a specific microphysics scheme. The code has many comments and it should be easy to modify it. This code also contains calls to NCAR-Graphics for plotting purposes. Either link to proper NCARG libraries or comment out the graphical portions of code. Please email W. Grabowski (grabow@ucar.edu) if you encounter any problems.

Example of results with a simple 1-moment bulk scheme without considering CCN processing obtained with the code available for download is shown in Fig. 2. The figure shows the quasi-steady solution from the kinematic model that is reached after a few hours (solution after one hour differs from the one showed in small details). As the figure shows, drizzle does not reach the surface in this case, but it should lead to changes in the CCN spectrum once such effects are included.

---

[1]https://raw.github.com/slayoo/icmw2012-case1/master/kinematic_wrain.vocals.f

4 Dynamic Model simulations

The dynamic model simulations should include key processes affecting the dynamics of the strato-cumulus-topped boundary layer (STBL), such as the cloud-top radiative cooling and surface water and energy fluxes that drive STBL circulations. It is left to the user to select the simulations framework (i.e., 2D versus 3D, specific domain size and gridlength). Below we present a setup that we used in a 2D simulation applying bulk microphysics without CCN processing. It is suggested that such a setup is used first to provide comparison with other participants. Subsequent tests should then explore the role of dimensionality, domain size, gridlength size, etc.

For the 2D dynamic model simulation, the computational domain is taken as 5 km in the horizontal (X) and 3 km in the vertical (Z). Model gridlength is taken to be (50,20) m in (X,Z). The model is driven by the cloud-top radiative cooling and by the surface fluxes. The radiative cooling is treated in a simplified way based on an approach developed by Stevens et al. (2005, eqs. 3 and 4 in particular). However, the free-tropospheric cooling is excluded and the local temperature tendency is derived from the divergence of the upward and downward fluxes given by

$$F_{rad}(x, z, t) = F_0 \exp(-Q(z, \infty) + F_1 \exp(-Q(0, z)))$$

$$Q(a, b) = \kappa \int_a^b \rho(q_c + q_r)dz$$

where, with $F_0 = 113\,Wm^{-2}$, $F_1 = 22\,Wm^{-2}$, $\kappa = 85\,m^2kg^{-1}$ (i.e., the latter two same as in Stevens et al. (2005), and ρ being the air density. Note that F_0 was increased from the value used in Stevens et al. (2005) (70 W m^{-2}) per Chris Bretherton's suggestion to match observations from VOCALS flights.

We purposely exclude large-scale subsidence that controls the depth of the boundary layer to avoid numerical issues with the subsidence implementation into the model. The increase of the boundary layer height can then be used as one of the measures of the simulated entrainment rate. This is consistent with excluding the free-tropospheric cooling included in Stevens et al. (2005) and omitted here. Surface latent and sensible heat fluxes are prescribed as 115 and 15 W m^{-2}, respectively. To ensure that the mean temperature and moisture profiles stay close to the initial profiles, a lower-boundary-layer relaxation similar to that used in the kinematic model is also applied in the dynamic model, but with a longer relaxation time scale, $\tau_{rlx} = 1800s$. Finally, to initiate boundary-layer circulations from motionless horizontally-uniform initial state, random temperature and moisture perturbations within the boundary layer (i.e., beneath 1500 m height) should be added. The amplitudes of the random perturbations should be 0.1 K and 0.2 g kg^{-1} for the potential temperature and water vapor mixing ratio.

The dynamic model is supposed to be run for 12 hours. It is suggested that the model is run for the first hour without drizzle formation to allow spinup of boundary-layer eddies.

Otherwise, significant drizzle develops at the onset in almost motionless atmosphere and leads to rapid thinning of the cloud layer. Note that this case features initially relatively deep boundary layer and deep cloud layer. Such conditions lead to the decoupling of the boundary layer (cf. Jones et al., 2011), an aspect that might play significant role in the dynamic model simulations, in contrast to the kinematic model where the flow is prescribed. Another aspect is that the interactions between dynamics and microphysics lead to solutions with significant temporal fluctuations of mean properties, as illustrated in Fig. 3. This is in contrast to the kinematic model results and may have some impact on the comparison between results using different microphysical schemes. Arguably, such fluctuations should be less pronounced in 3D models.

The emphasis of the analysis should be on the evolution of mean properties characterizing cloud and precipitation processes, such as the mean cloud depth and cloud water path, the mean cloud droplet concentration and surface precipitation rate, as well as the evolution of the CCN characteristics (mean concentration, mean radius and mass, etc). Note that possibly significant difference between kinematic and dynamic model simulations in the cloud-top entrainment, present only in the dynamic model simulations. This aspects can be one of the foci of the intercomparison between results from the two models.
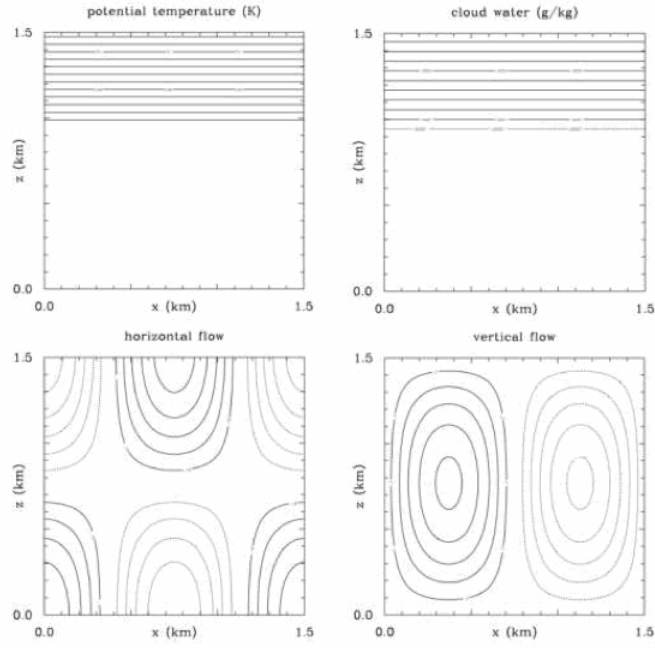
Figure 1: (Upper panels) Initial fields of the potential temperature and cloud water mixing ratio resulting from the decomposition of the initial profiles of the liquid water potential temperature and total water. (Lower panels) Constant in time horizontal and vertical velocities used in the kinematic test case. Contour intervals are 0.2 K, 0.1 $\mathrm{g\,kg^{-1}}$ for the temperature and liquid water, and $0.1/0.2\ \mathrm{m\,s^{-1}}$ for the horizontal/vertical velocity.
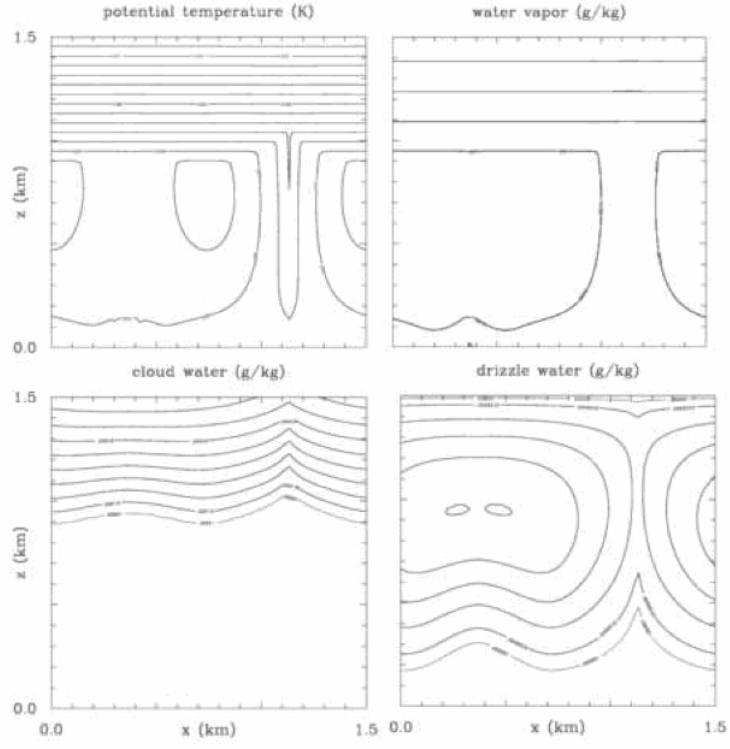
Figure 1:

Figure 2: Quasi-steady solutions from the kinematic model. Contour intervals are 0.1 K, 0.25 g kg^{-1}, 0.1 g kg^{-1} and 0.002 g kg^{-1} for the temperature, water vapor, cloud water, and drizzle water.
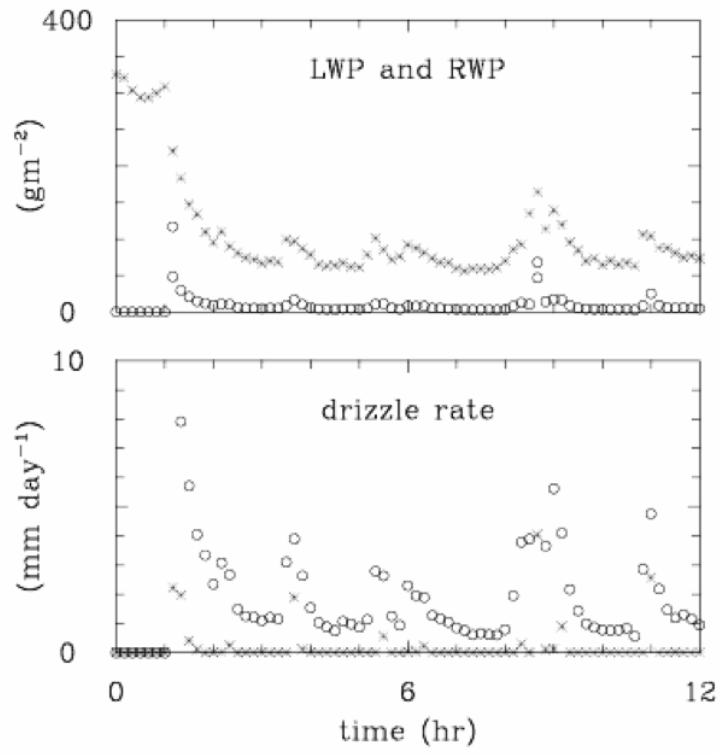
Figure 2:

Figure 3: Evolution of the domain-averaged liquid water and rain-water paths (LWP and RWP, starts and circles, respectively)) and corresponding precipitation rates at 1-km height and at the surface (circles and stars, respectively) for a 2D STBL simulation applying a simple bulk scheme.

Figure 3:

References

Allen, G., Coe, H., Clarke, A., Bretherton, C., Wood, R., Abel, S. J., Barrett, P., Brown, P., George, R., Freitag, S., McNaughton, C., Howell, S., Shank, L., Kapustin, V., Brekhovskikh, V., Kleinman, L., Lee, Y.-N., Springston, S., Toniazzo, T., Krejci, R., Fochesatto, J., Shaw, G., Krecl, P., Brooks, B., McMeeking, G., Bower, K. N., Williams, P. I., Crosier, J., Crawford, I., Connolly, P., Allan, J. D., Covert, D., Bandy, A. R., Russell, L. M., Trembath, J., Bart, M., McQuaid, J. B., Wang, J., and Chand, D.: South East Pacific atmospheric composition and variability sampled along 20S during VOCALS-REx, Atmos. Chem. Phys., 11, 5237–5262, 2011.

Flossmann, A. I. and Wobrock, W.: A review of our understanding of the aerosol-cloud interaction from the perspective of a bin resolved cloud scale modelling, Atmos. Res., 97, 478–497, 2010.

Jones, C. R., Bretherton, C. S., and D.Leon: Coupled vs. decoupled boundary layers in VOCALS-REx, Atmos. Chem. Phys., 11, 7143–7153, 2011.

Stevens, B., Moeng, C.-H., Ackerman, A. S., Bretherton, C. S., Chlond, A., de Roode, S., Edwards, J., Golaz, J.-C., Jiang, H., Khairoutdinov, M., Kirkpatrick, M. P., Lewellen, D. C., Lock, A., Müller, F., Stevens, D. E., Whelan, E., and Zhu, P.: Evaluation of Large-Eddy Simulations via observations of nocturnal marine stratocumulus, Mon. Wea. Rev., 133, 1443–1461, 2005.

Wood, R., Bretherton, C. S., Leon, D., Clarke, A. D., Zuidema, P., Allen, G., and Coe, H.: An aircraft case study of the spatial transition from closed to open mesoscale cellular convection over the Southeast Pacific, Atmos. Chem. Phys., 11, 2341–2370, 2011.